



Integrated approach for the development across Europe of user oriented climate indicators for GFCS high-priority sectors: Agriculture, disaster risk reduction, energy, health, water and tourism

Work Package 6

Deliverable 6.4

# Report on the assessment of sectorial climate change impact based on INDECIS-ISD in the context of climate change scenarios (UC-IH contribution)

Joaquin Bedia, Ana Casanueva, Juan Antonio Fernández Granja, Sixto Herrera, Manuel del Jesús, Javier Díez Sierra



This report arises from the Project INDECIS which is part of ERA4CS, an ERA-NET initiated by JPI Climate, and funded by FORMAS (SE), DLR (DE), BMWFW (AT), IFD (DK), MINECO (ES), ANR (FR), with co-funding by the European Union's Horizon 2020 research and innovation programme



# Abstract

We present future climate change projections for three INDECIS-ISD indices representative of extremes for precipitation (Rx1day), maximum (XTX) and minimum (NTN) temperatures, using an ensemble of state-of-the-art RCM simulations from EURO-CORDEX. To this aim, we compute delta change maps using the reference CMIP5 historical period (1986-2005) and two future time slices (mid term, 2021-2050) and long-term (2071-2100), analysing the projections for RCPs 4.5 and 8.5.

Overall results indicate a strong positive signal for the temperature-related extremes in all seasons, with a projected increment of minimum temperatures particularly accentuated in the northern part of Europe (Scandinavia) in winter, and strong increments of hot extremes in the Mediterranean during the summer. Regarding extreme precipitation, an overall increase is projected over most of the continent throughout the year, except for the Iberian Peninsula in spring and autumn (also Italy in spring) and the Mediterranean region in summer. However, model uncertainty is large, since the multi-model spread is similar to or larger than the signals. Overall, the largest impacts are expected as a result of the strong positive signals projected for extreme heat, as characterized by XTX, for which a special focus is undertaken in our discussion.

## Introduction

The assessment of climate change impacts in coastal areas and regions with complex orography poses a challenge related to shortcomings of the Global Climate Models (GCMs). The use of dynamically downscaled projections can help to reduce the regional uncertainties and to provide more accurate results for specific regions. In this deliverable, we show future climate projections of three selected INDECIS ISD indices representative of hot, cold and precipitation extremes using Regional Climate Model (RCM) simulations from the EURO-CORDEX project (Jacob *et al.* 2014, Kotlarski *et al.* 2014).

EURO-CORDEX is the European branch of the CORDEX initiative, which is a program sponsored by the World Climate Research Program (WRC) to organize an internationally coordinated framework to produce improved regional climate change projections for all land regions world-wide, building upon an ensemble of GCM-RCM couplings. EURO-CORDEX oversees the design and coordination of ongoing ensembles of regional climate projections of unprecedented size (to date more than 150 simulations, from more than 30 modelling groups) and resolution (0.11° and 0.44° horizontal resolutions). The value of the EURO-CORDEX ensemble has been shown via numerous peer-reviewed studies (Jacob *et al.* 2020) and its use in the development of climate services. The increased resolution with respect to the global counterparts can be regarded as an added value of regional climate simulations (Torma *et al.* 2015). The results of the newer EURO-CORDEX ensemble strengthen those obtained in the previous GCM-RCM intercomparison project ENSEMBLES (van der Linden and Mitchell 2009) regarding temperature changes. Small signals are found for precipitation, although the new generation of RCM simulations exhibit an added value by providing higher daily precipitation intensities, which are mostly missing in the

global climate model simulations. Moreover, the state-of-the-art projections provide a significantly different climate change of daily precipitation intensities resulting in a smoother shift from weak to moderate and high intensities (Jacob *et al.* 2020, Soares and Cardoso 2020).

Different nature thresholds are typically used to quantify extremes and their impacts, therefore robust methodologies are needed in order to produce reliable climate change projections. Despite the common use of percentile-based indices, they have little bearing on impacts on human activities and agricultural products (Grotjahn 2020). Consequently, many impact studies rely on absolute exposure limits. As an example, absolute temperature thresholds play an important role in climate services provision. Furthermore, the assessment of impacts in regions with complex orography, intricate coastlines and/or small islands poses a challenge related to the inherent shortcomings of Global Climate Models (GCMs), related to their coarse spatial resolution and limited ability to model small-scale processes which depend on the orography and land-sea interactions (see e.g. Sanjay *et al.* 2017, Karl *et al.* 1999, Peterson *et al.* 2002). These problems are partially alleviated by the higher resolution and better resolved processes of the RCMs. However, systematic biases remain. The application of some sort of bias adjustment (BA) can alleviate this problem and becomes essential when absolute thresholds are examined (e.g. Zhao *et al.* 2015, Dosio 2016, Matthews *et al.* 2017, Li *et al.* 2020). BA thus serves to place all models on equal footing, at the expense of some additional uncertainty due to the adjustment method (Casanueva *et al.* 2020a, Iturbide *et al.* 2020). In this deliverable we skip this added source of uncertainty by using a subset of INDECIS-ISD indices (Table 1) which do not depend on absolute thresholds. Instead, they are relative to each model's maximum/minimum precipitation/temperature values, in order to gain an insight into the likely future impacts. As long as climate change signals are considered, systematic biases on a given percentile cancel out since the deltas are computed relative to the historical period for each GCM-RCM (Table 2). Thus, the presented results correspond to the original, raw model outputs, without bias adjustment.

## Data and Methods

### *Index selection and calculation procedure*

We consider three INDECIS-ISD indices representative of potential changes in extreme precipitation (Rx1day), extreme heat (XTX) and extreme cold (NTN), that are calculated upon the daily time series of the following Essential Climate Variables (ECVs, Table 1): precipitation, maximum near-surface (2m) temperature and minimum near-surface (2m) temperature, respectively. The original monthly index values are then seasonally aggregated as the seasonal maximum, maximum and minimum values respectively. The climate change signals (deltas) are computed as the difference between the future (mid term, 2021-2050, and long-term, 2071-2100) and the historical climatologies, considering the standard baseline period of CMIP5 (1986-2005, Taylor *et al.* 2012).

As stated in the introduction, the chosen indices do not require bias adjustment because the deltas are calculated using data from each model separately, therefore, systematic biases cancel out. Thus, the presented ensemble projections avoid the added uncertainty associated with the bias correction method, required for other threshold-dependent indices.

ISD*	Index Code	ECV	Description
2	XTX	Maximum temperature	Maximum value of monthly maximum air temperature
6	NTN	Minimum temperature	Minimum value of monthly minimum air temperature
47	Rx1day	Precipitation	Monthly maximum 1-day precipitation

**Table 1.** INDECIS ISD subset used for the assessment of climate change. \*The ISD numbers correspond to the index description provided in INDECIS D4.1 (“Report on the Inventory and Catalog of Indices Datasets”) and INDECIS D4.2 (“Report on Indices of INDECIS-ISD, including definitions, and accompanying sectorial data”), where further details in these indices can be found.

The indices have been calculated using the R package [climate4R.indices](#), implementing several INDECIS ISD and indicators of circulation variability within the [climate4R framework](#) for climate data access, processing and visualization (Frías *et al.* 2018, Iturbide *et al.* 2019).

### *RCM-GCM ensemble*

A subset of the EURO-CORDEX (Jacob *et al.* 2014, Kotlarski *et al.* 2014) multimodel ensemble (16 GCM-RCM couples stemming from 13 GCMs and 7 RCMs, see Table 2) has been chosen considering the availability of data for both RCPs (4.5 and 8.5) for full comparability among indices and experiments. For instance, to date RCP4.5 is not available for CCLM5-0-6 v1, therefore all the GCM-RCM couples corresponding to this RCM have been discarded for this analysis for full comparability of results. Note the uneven distribution of the models within the matrix (e.g. 9 out of the 16 couples correspond to

RCA4\_v1). Still, the multimodel ensemble mean is derived from all available simulations, with no special weighting. Only simulations at 0.44° resolutions are used.

	CCLM4-8-17_v1	ALADIN53_v1	WRF331F_v1	RACMO22_E_v1	RACMO22_E_v2	REMO2009_v1	RCA4_v1
MPI-ESM-LR_r1i1p1	X					X	X
MPI-ESM-LR_r2i1p1						X	
CNRM-CM5_r1i1p1		X					
EC-EARTH_r1i1p1				X			
EC-EARTH_r12i1p1							X
MIROC5_r1i1p1							X
HadGEM2-ES_r1i1p1					X		X
CinquiniiPSL-CM5A-MR_r1i1p1			X				
CanESM2_r1i1p1							X
CSIRO-Mk3-6-0_r1i1p1							X
CM5A-MR_r1i1p1							X
NorESM1-M_r1i1p1							X
ESM2M_r1i1p1							X

**Table 2.** GCM(rows)-RCM(columns) matrix of the EURO-CORDEX multi-model ensemble considered in this study. The ensemble is complete, i.e., for all the GCM-RCM pairs both RCP 4.5 and 8.5 all indices are available.

## Regridding

All the indices have been computed using the native RCM grids as delivered through ESGF (Cinquini et al. 2014, <https://esgf.llnl.gov>) at a horizontal resolution of 0.44°. After the index calculation, all data have been re-gridded onto a regular 0.5 degree resolution grid (as displayed in the figures) to build the ensemble results, using a first-order conservative remapping approach. The use of this grid is aligned with the IPCC-WG1 Atlas products, to be delivered for AR6, publicly available in the Atlas repository (<https://github.com/SantanderMetGroup/ATLAS/tree/master/reference-grids>). Conservative mapping methods attempt to preserve fluxes (or other integrals) during the interpolation process (in particular precipitation). The method is also applied to temperatures (and temperature-related indices) in order to have full comparability of results among variables. This conservative remapping approach has been used in the framework of the EURO-CORDEX project. The basic remapping operand is conservative remapping as defined in CDO (Schulzweida 2018).

The regridding procedure has the following characteristics:

1. Variables exposing a large sensitivity to land-sea contrast are remapped with reference to land-sea mask in the native grid and the regular grid. This includes virtually all (near-) surface variables. In this study, the indices using the land-sea contrast are NTN and XTX, for which a sharp land-sea transition is assumed.
2. A common land-sea fraction (sftlf) regular reference grid is employed. NetCDF files containing such information at both input/output resolutions have been prepared for that aim.
3. Variables not categorized in step (1) are remapped straightforwardly with disregard of land sea mask. In this study, this refers to Rx1day, as long as precipitation does not exhibit a strong land-sea contrast.
4. Isolated islands or lakes in the regular grid (typically sized at grid cell mesh) which are not represented in the native grid will not be processed in step (2).

Therefore, regarding the land-sea contrast: first interpolation is done over land, then over sea, and lastly over the whole area. Afterwards, the interpolated sea and land are merged, after which some missing values will appear along the coastlines. These areas will be filled with the data from the "whole area" interpolation. As result, in conservative remapping the variables that are sensitive to land-sea transitions are dually interpolated, i.e. land-sea separated, and then re-combined in one file. Residual missing values (NaN) in the interior domain are filled with values from a straightforward remap. The regridding procedure is further detailed in the following link, that also contains the necessary code and input grids to reproduce the interpolation step:

[https://github.com/SantanderMetGroup/ATLAS/tree/mai-devel/SOD-scripts/bash-interpolation-scripts/AtlasCDOremapper\\_CORDEX](https://github.com/SantanderMetGroup/ATLAS/tree/mai-devel/SOD-scripts/bash-interpolation-scripts/AtlasCDOremapper_CORDEX)

# Results

## *Reference values for sectoral indices*

The analysis of the reference values of sectoral indices in the period 1986-2005 provides the starting point for the delta changes and related uncertainties. The largest values of Rx1day occur in western Scandinavia, northwestern Iberian Peninsula and the main mountain ranges (Alps, Pyrenees, Carpathians and Dinaric Alps) in winter and autumn, with Rx1day of approximately 50-70mm/d (Fig.1, left). The main flow regimes in winter, dominated by advection from the west and northwest, and a southerly flow of humid Mediterranean air in autumn can explain such precipitation extremes (CH2018, 2018). Rx1day values decrease gradually from winter to spring and from spring to summer. The largest values in spring and summer are found in the main mountain ranges (40-60mm/d) and might be explained by convection activity. The multi-model spread is below 10mm/d in large parts of the continent but it reaches up to 20 and 30 mm/d in the southern Alpine rim in winter and autumn, respectively (Fig. 1, right).

Temperature extremes present a north-south gradient and orographic pattern, with larger XTX and NTN southwards and lower values in the north and the mountainous areas. XTX is above 35°C in spring and summer and between 22°C-30°C in autumn in large parts of the center and south of the continent (Fig. 2, left). Minimum temperature extremes (NTN) are found in the Scandinavian Peninsula and the Alps with values well below -30°C in winter, between -30°C to -20°C in spring, between -22°C to -15°C in autumn and above -5°C in summer (Fig.3, left). In the rest of Europe, NTN varies between -22 and 0°C in winter, -14°C and 4°C in spring, 2 to 10°C in summer and -8°C to -4°C in autumn. Model uncertainty is small for temperature extremes in the historical scenario (Fig.2 and 3, right panels), being below 5°C except for NTN in spring and winter in northern Europe, where it amounts up to 10°C.

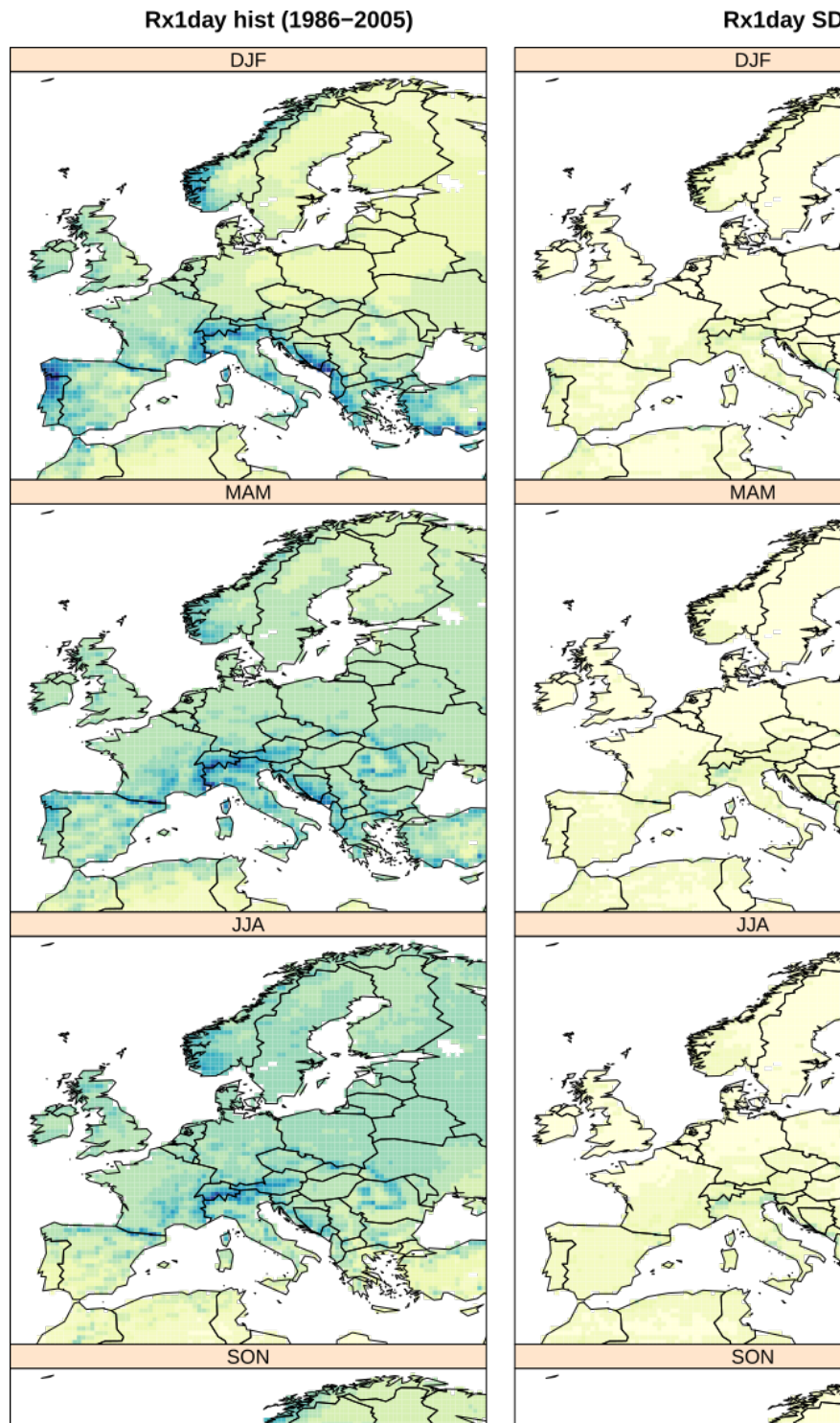


**Fig. 1.** Left: EURO-CORDEX multimodel ensemble mean (n=16) seasonal climatologies of the Rx1day index (mm/d) as simulated by the historical experiment for the period 1986-2005. Right: Multimodel spread, represented by its standard deviation.

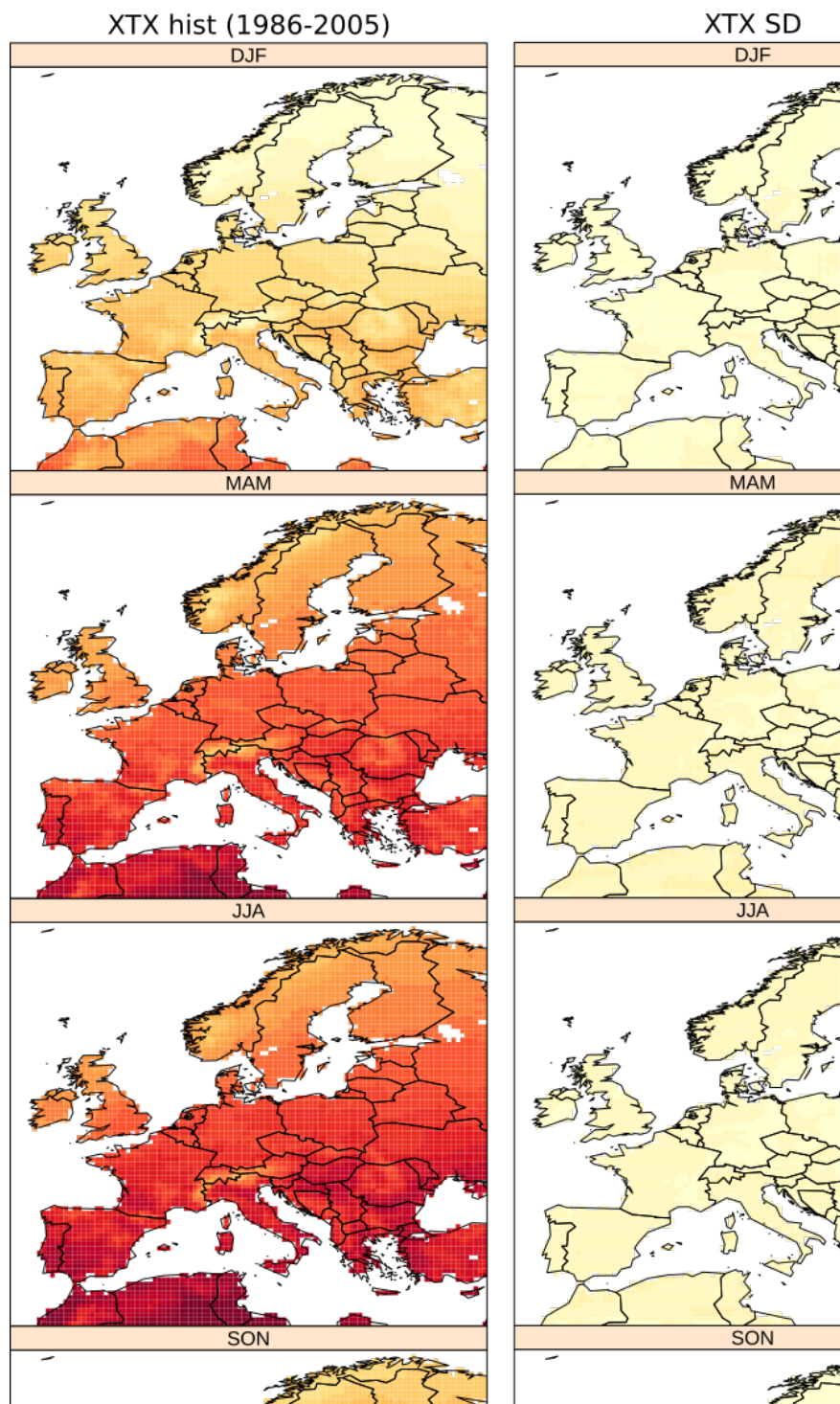


**Fig. 2.** Left: EURO-CORDEX multimodel ensemble mean (n=16) seasonal climatologies of the XTX index (°C) as simulated by the historical experiment for the period 1986-2005. Right: Multimodel spread, represented by its standard deviation.

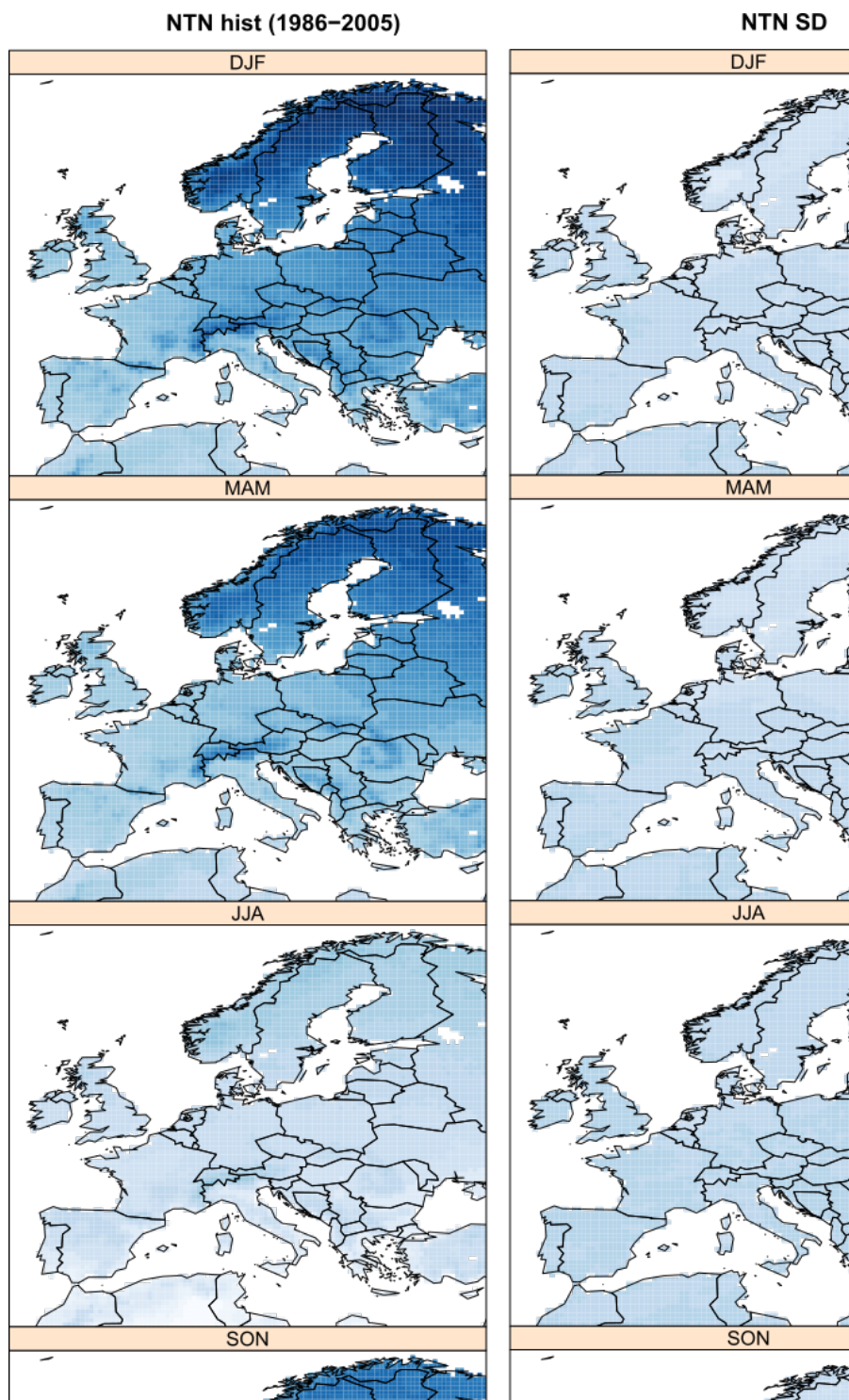


**Fig. 3.** Left: EURO-CORDEX multimodel ensemble mean (n=16) seasonal climatologies of the NTN index (°C) as simulated by the historical experiment for the period 1986-2005. Right: Multimodel spread, represented by its standard deviation.

## *Climate change signals of sectoral indices*

Climate change projections of Rx1day indicate a continuous increase along the four seasons in large parts of the continent, which amounts to 2-4mm/d by mid-century and 6-9mm/d towards the end of the century (Fig.4). The increase is projected to affect most of the continent, except for the Iberian Peninsula in spring and autumn (also Italy in spring) and the Mediterranean region in summer. Indeed, some drying is projected over the Iberian Peninsula and the Alps towards the end of the century, especially in summer (up to 6mm/d less). Multi-model spread is large, mostly similar to or even larger than the projected signals, especially in the regions with higher historical records. Large discrepancies among models are also found in the regions where a summer reduction of Rx1day is projected. Results for the intermediate emission scenario (RCP 4.5) are similar to those for RCP8.5 for mid-century, with a clear stabilization towards the end of the century (Fig. A1).

Extreme maximum temperatures are projected to increase up to 2.5°C evenly across Europe throughout the year by mid-century (Fig.5, left). Changes accentuate towards the end of the century in southern Europe in spring and autumn and extend to Central Europe in summer (increases of up to 6°C, Fig.5, right). Interestingly, increments of about 5-6°C are also found in the Scandinavian Peninsula in spring and in the Alps and the Carpathians in winter. Overall, model agreement is large, with an ensemble spread of less than 2°C in most of the cases (note slightly higher values in Scandinavia and the Alps in spring).

Unlike changes of XTX, which are featured in the south of the continent, NTN is projected to increase to a greater extent in northern and north-eastern Europe (Fig.6), which are precisely the regions with the lowest NTN. These increments amount to 2-7°C by mid-century and 8-12°C by the end of the century throughout the year except in summer (increments of up to 2°C for mid-century and 5°C by the end of the century). In winter, the notable increase of NTN is evident in most of the continent, except for the Mediterranean region and the British Isles. As for XTX, multi-model uncertainty is small (below 2°C), except for some areas in Scandinavia in winter and spring (up to 5°C).

As for precipitation, the two scenarios become more distinct by the end of the century, with the largest increases of XTX ranging between 3-4°C (Fig. A2) and NTN between 6-8°C (Fig. A3), whilst keeping the same spatial pattern as for RCP8.5 across seasons.

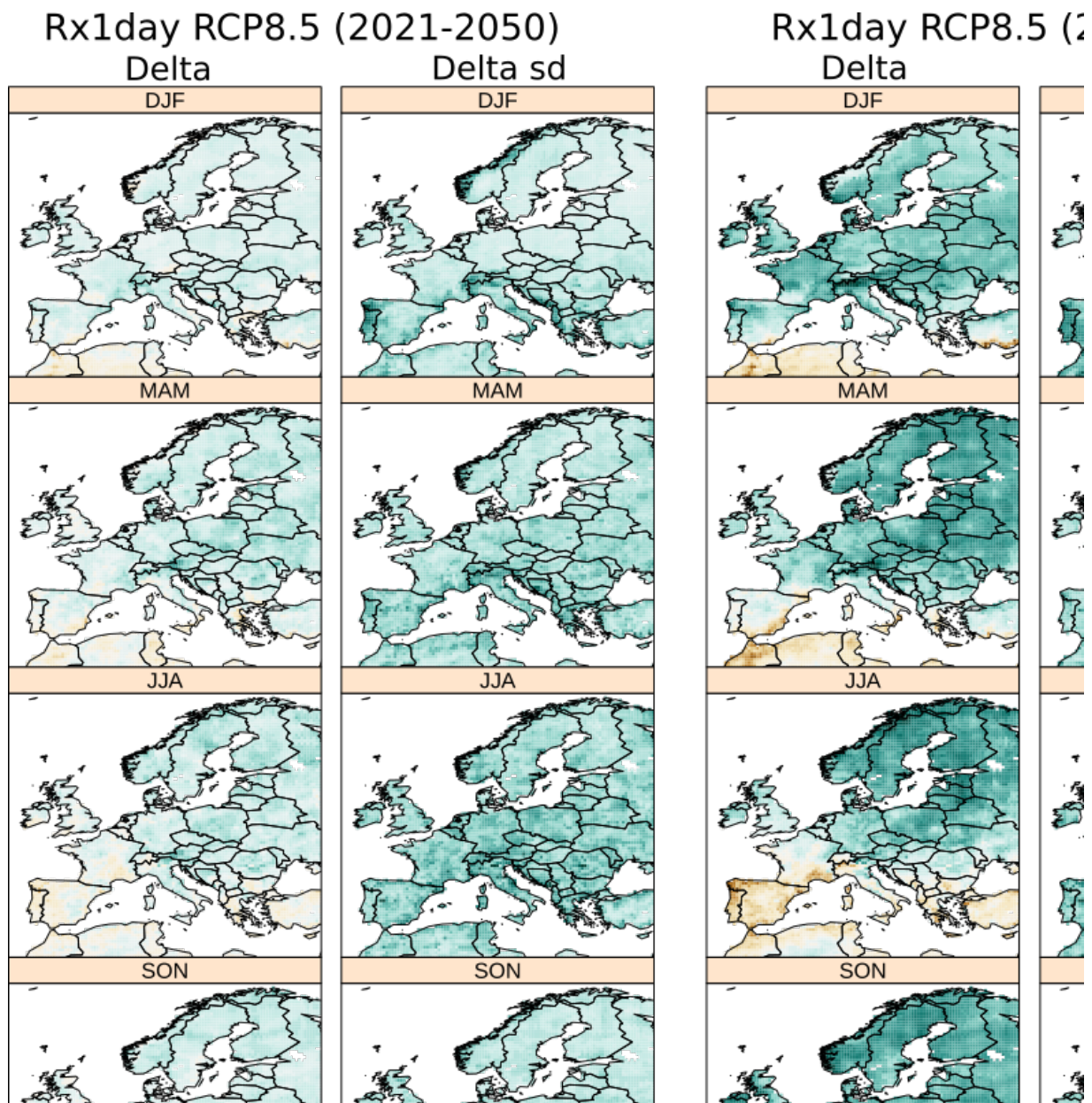


**Fig. 4.** First and third columns: Delta maps of Rx1Day considering the periods 2021-2050 and 2071-2100, respectively, for RCP 8.5 against the historical baseline 1986-2005. Second and fourth columns: standard deviation of the deltas for their respective periods.

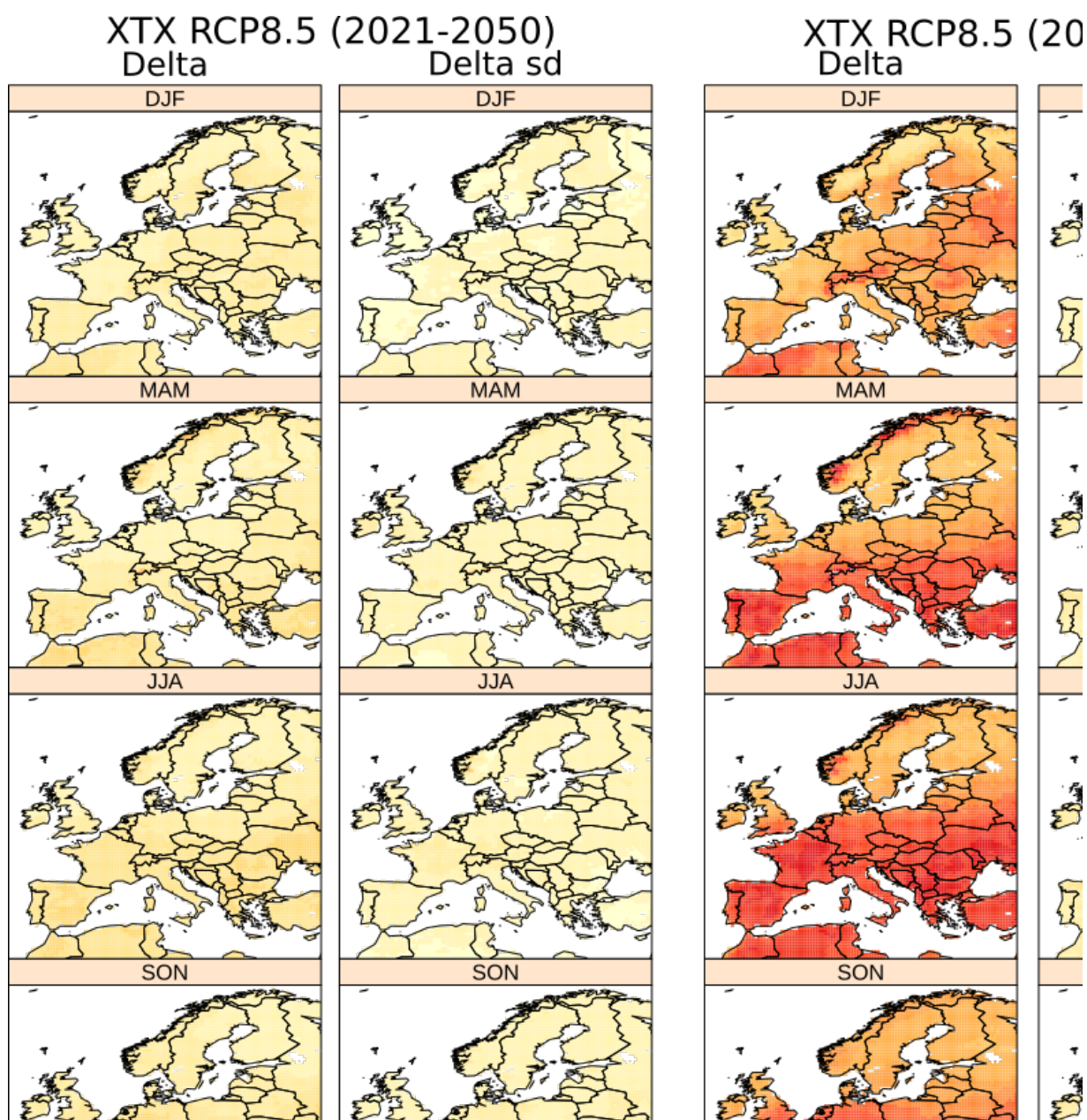


**Fig. 5.** First and third columns: Delta maps of XTX considering the periods 2021-2050 and 2071-2100, respectively, for RCP 8.5 against the historical baseline 1986-2005. Second and fourth columns: standard deviation of the deltas for their respective periods.

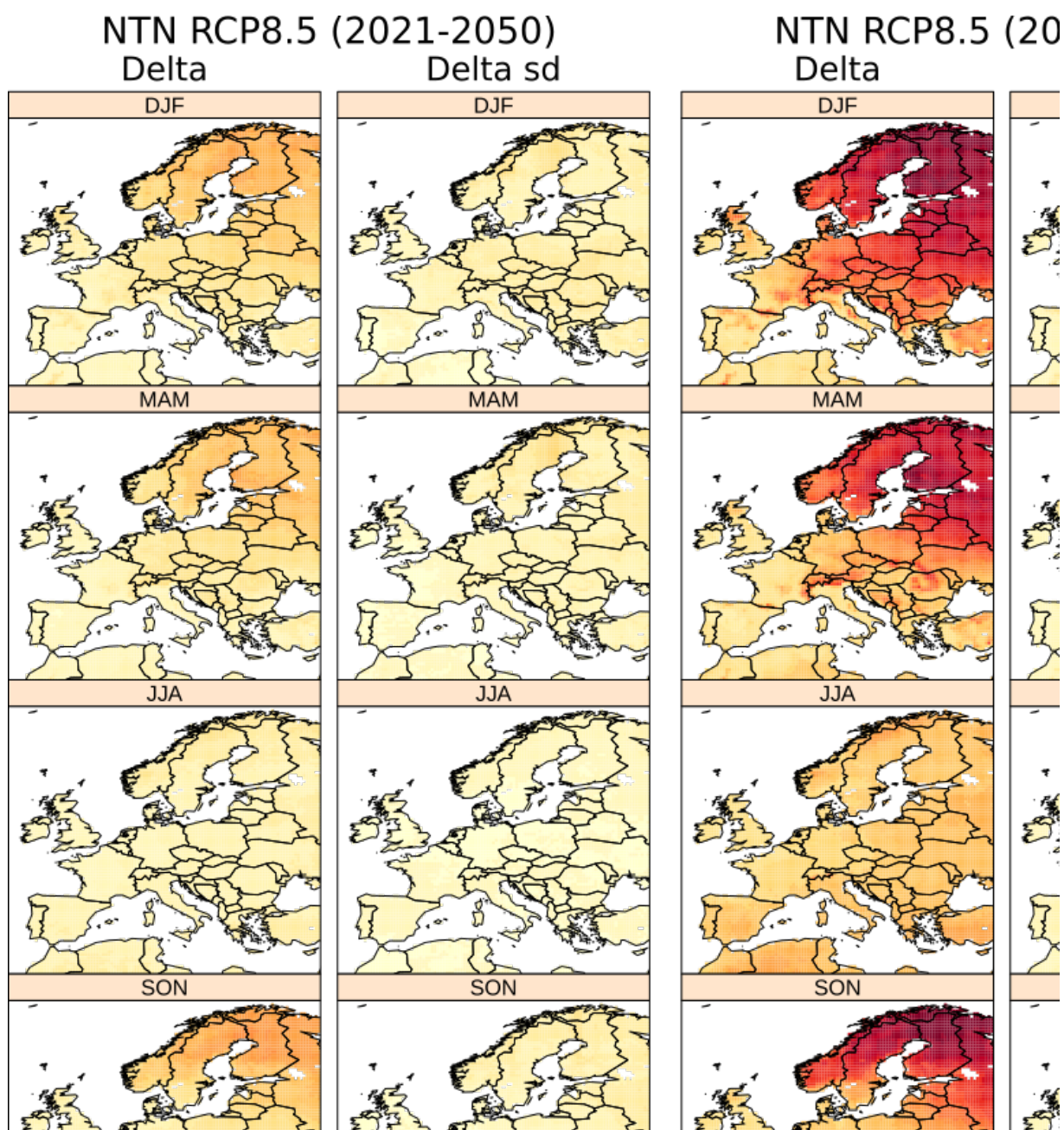


**Fig. 6.** First and third columns: Delta maps of NTN considering the periods 2021-2050 and 2071-2100, respectively, for RCP 8.5 against the historical baseline 1986-2005. Second and fourth columns: standard deviation of the deltas for their respective periods.

## *Sectoral climate change impacts based on the selected indices*

The projected changes of the considered climate indices have many implications in different impact sectors. As described in the INDECIS deliverable 4.2, Rx1day is relevant for agriculture and water resources and the temperature extremes (XTX and NTN) for agriculture, tourism, water resources and human health. Despite the large increments for Rx1day, we refrain from elaborating further interpretations given the large multi-model uncertainty and focus on the temperature extremes.

The negative impacts of extremely high temperatures are remarkable on human well-being, human activities, ecosystems and biodiversity. The results shown in the previous section suggest that large areas of the continent might suffer from substantial increases in the highest temperature during day and the lowest during night. Hereafter, some of the related impacts of such changes are examined.

The consequences of major heat waves for human health have become apparent from the fatalities of recent events such as the 2003 heatwave in Europe (more than 70,000 excess deaths across 12 European countries - Robine *et al.* 2008 -, and economic losses amounted to more than 13 billion euros - de Bono *et al.* 2004) and the 2010 heatwave in Russia (Barriopedro *et al.* 2011). Currently the human thermoregulatory capacity of around a quarter of the world's population is affected by climate and such climatic conditions are projected to increase with increasing green-house gas emissions especially in the humid tropics (Mora *et al.* 2017).

The exposure-response relationship between temperature and heat-related impacts are usually built by either identifying “trigger points” or exposure limits linked, for instance, to the increased risk of health events (mortality, hospitalizations) associated directly and indirectly with heat (Petitti *et al.* 2016) or analyzing the health outcomes in days which are *a priori* defined (e.g. surpassing a threshold or specific climatological percentile - Ragetli *et al.* 2017). The variety of such limits for a particular application is large, e.g. trigger points related to mortality are consistently higher than those for other relevant health events (e.g. hospitalizations and heat-related illnesses - Petitti *et al.* 2016). Staying below certain exposure limits (e.g. ambient temperature below 35°C - Kjellstrom *et al.* 2009a - and core body temperature below 38°C - Kjellstrom *et al.* 2009b) reduces the risk of heat-related illnesses, but does not preclude the possibility of other adverse effects such as a loss of labour productivity (Casanueva *et al.* 2020b). The individuals' natural response to protect themselves against the risk of heat-related illnesses is to slow down the intensity of the activity/work and/or limit working hours, thus minimizing body heat production and reducing heat exposure, respectively (Ioannou *et al.* 2017). As a consequence of these strategies, labour productivity and economic output are reduced (Kjellstrom *et al.* 2018, Orlov *et al.* 2019). For instance, Dunne *et al.* 2013 found a reduction in labour capacity to less than 40% by 2200 in peak months, with most tropical and mid-latitude regions experiencing extreme heat stress, under the strongest emission scenario. Likewise southern Europe might experience a widespread loss of

working hours by at least 15%, reaching more than 50% in some locations in Spain, Italy, Greece and Cyprus by the end of the 21st century under RCP8.5 (Casanueva *et al.* 2020b).

Excessive heat has also an impact on biodiversity and crop yields, with large or small impacts depending on the development stage of the plant (Grotjahn 2020). In particular, the negative impact of heat during the reproductive stage of the crops is a major threat to yield in many parts of the world (Deryng *et al.* 2014, Hatfield and Prueger 2015). Deryng *et al.* 2014 found strong heat stress effects for maize, which are responsible for up to 45% of global average yield losses, and spring wheat, responsible for up to 52% reduction of global average yield gains, under RCP8.5 by the 2080s relative to the 1980s. Furthermore, maize pollen viability decreases with temperatures above 35°C and rice production ceases above 40°C (Hatfield and Prueger 2015, Grotjahn 2020 and references therein). Beyond damages in crop yields, high temperatures are associated with greater water usage, e.g. maize water demand doubles as temperatures increase from 27°C to 35°C (Grotjahn 2020).

According to the IPCC (IPCC 2019), the observed global warming has led to widespread shrinking of the cryosphere, with mass loss from ice sheets and glaciers (very high confidence), reductions in snow cover (high confidence) and increased permafrost temperature (very high confidence). Our results show a large and robust projected increase of NTN (winter, spring, autumn) and XTX (spring and summer) in typically cold European regions such as Scandinavia and the Alps. In light of this situation, glacier mass loss, permafrost thaw and decline in snow cover might continue in the next decades, with an increasing rate throughout the 21st century. These might have unavoidable consequences for river runoff, local hazards and terrestrial and freshwater ecosystems (IPCC 2019).

Limiting global warming to 1.5°C is essential to mitigate all the above mentioned effects of extreme heat conditions (Lo *et al.* 2019).

## Conclusions

This work shows climate change projections of three climate indices describing extreme precipitation and temperatures using a large ensemble of EURO-CORDEX regional climate models driven by CMIP5 global climate models under two different scenarios (RCP 4.5 and 8.5). Our results suggest that large areas of Europe might suffer from substantial increases in the highest temperature during day (XTX) and the lowest during night (NTN). Changes of XTX accentuate towards the end of the century in southern Europe in spring and autumn and extend to Central Europe in summer, whereas NTN is projected to increase to a greater extent in northern and north-eastern Europe, which are precisely the regions with the lowest NTN. These non-linear increments in the tails of the temperature distribution highlight even further the need to investigate the negative impacts of extremely high temperatures, which are remarkable on human well-being, human activities, ecosystems and biodiversity.

Highest 1-day precipitation (Rx1day) is selected to account for extreme precipitation. Rx1day is projected to increase continuously along the four seasons in large parts of the continent, except for the Iberian Peninsula in spring and autumn (also Italy in spring) and the Mediterranean region in summer. The increase of Rx1day might be related to an intensification of the hydrological cycle associated with a warming-related increase of atmospheric moisture content (Schmidli et al., 2007 and references therein). This is in agreement with the Clausius–Clapeyron relation that describes how a warmer atmosphere can hold more water vapour, which produces in turn more intense precipitation. We found, however, large ensemble spread relative to the signals.

## References

Barriopedro, D., Fischer, E. M., Luterbacher, J., Trigo, R. M. and García-Herrera, R. (2011) The hot summer of 2010: Redrawing the temperature record map of Europe. *Science*, 332, 220–224.

Casanueva, A., Herrera, S., Iturbide, M., Lange, S., Jury, M., Dosio, A., Maraun, D. and Gutiérrez, J.M. (2020a) Testing bias adjustment methods for regional climate change applications under observational uncertainty and resolution mismatch. *Atmospheric Science Letters*, 21, e978.

Casanueva, A., Kotlarski, S., Fischer, A. M., Flouris, A. D., Kjellstrom, T., Lemke, B., Nybo, L., Schwierz, C. and Liniger, M. A. (2020b) Escalating environmental summer heat exposure: a future threat for the European workforce. *Regional Environmental Change*, 20, <https://doi.org/10.1007/s10113-020-01625-6>

CH2018 (2018), CH2018 – Climate Scenarios for Switzerland, Technical Report, National Centre for Climate Services, Zurich, 271 pp. ISBN: 978-3-9525031-4-0.

Cinquini, L., Crichton, D., Mattmann, C., Harney, J., Shipman, G., Wang, F., Ananthkrishnan, R., Miller, N., Denvil, S., Morgan, M., Pobre, Z., Bell, G.M., Doutriaux, C., Drach, R., Williams, D., Kershaw, P., Pascoe, S., Gonzalez, E., Fiore, S., Schweitzer, R., 2014. The Earth System Grid Federation: An open infrastructure for access to distributed geospatial data. *Future Generation Computer Systems*, Special Section: Intelligent Big Data Processing 36, 400–417. <https://doi.org/10.1016/j.future.2013.07.002>

De Bono, A., Giuliani, G. and Kluser, S. and Peduzzi, P. (2004) Impacts of summer 2003 heat wave in Europe. Tech. Rep. 1-4, United Nations Environment Programme.

Deryng, D., Conway, D., Ramankutty, N., Price, J. and Warren, R. (2014) Global crop yield response to extreme heat stress under multiple climate change futures. *Environmental Research Letters*, 9, 034011.

Dosio, A. (2016) Projections of climate change indices of temperature and precipitation from an ensemble of bias-adjusted high-resolution EURO-CORDEX regional climate models. *Journal of Geophysical Research—Atmospheres*, 121, 5488–5511. <https://doi.org/10.1002/2015JD024411>

Dunne JP, Stouffer RJ, John JG (2013) Reductions in labour capacity from heat stress under climate warming. *Nat Clim Chang* 3:563–566. <https://doi.org/10.1038/nclimate1827>

Frías, M.D., Iturbide, M., Manzanas, R., Bedia, J., Fernández, J., Herrera, S., Cofiño, A.S., Gutiérrez, J.M., 2018. An R package to visualize and communicate uncertainty in seasonal climate prediction. *Environmental Modelling & Software* 99, 101–110. <https://doi.org/10.1016/j.envsoft.2017.09.008>

Grotjahn, R. (2020) Weather extremes that impact various agricultural commodities. In [Castillo, F. and Wehner, M. and Stone, D. (eds.)] *Extreme Events and Climate Change: A Multidisciplinary Approach*. John Wiley & Sons, Inc. for American Geophysical Union. In press.

Hateld, J. L. and Prueger, J. H. (2015) Temperature extremes: Effect on plant growth and development. *Weather and Climate Extremes*, 10, 4 – 10. USDA Research and Programs on Extreme Events.

Ioannou LG, Tsoutsoubi L, Samoutis G, Bogataj LK, Kenny GP, Nybo L, Kjellstrom T, Flouris AD. (2017) Time-motion analysis as a novel approach for evaluating the impact of environmental heat exposure on labor loss in agriculture workers. *Temperature (Austin)* 4(3):330-340. DOI: 10.1080/23328940.2017.1338210. PMID: 28944274; PMCID: PMC5605156.

Iturbide, M., Gutiérrez, J.M., Alves, L.M., Bedia, J., Gimadevilla, E., Cofiño, A.S., Cerezo-Mota, R., Di Luca, A., Faria, S.H., Gorodetskaya, I., Hauser, M., Herrera, S., Hewitt, H.T., Hennessy, K.J., Jones, R.G., Krakovska, S., Manzanas, R., Marínez-Castro, D., Narisma, G.T., Nurhati, I.S., Pinto, I., Seneviratne, S.I., van den Hurk, B., Vera, C.S., 2020. An update of IPCC climate reference regions for subcontinental analysis of climate model data: Definition and aggregated datasets. *Earth System Science Data Discussions*. <https://doi.org/10.5194/essd-2019-258>

Iturbide, M., Casanueva, A., Bedia, J., Herrera, S., Milovac, J. and Gutiérrez, J.M. (2020). On the need of bias adjustment for more plausible climate change projections of extreme heat. *Atmospheric Science Letters*, *submitted*.

Iturbide, M., Bedia, J., Herrera, S., Baño-Medina, J., Fernández, J., Frías, M.D., Manzanas, R., San-Martín, D., Gimadevilla, E., Cofiño, A.S., Gutiérrez, J.M., 2019. The R-based climate4R open framework for reproducible climate data access and post-processing. *Environmental Modelling & Software* 111, 42–54. <https://doi.org/10.1016/j.envsoft.2018.09.009>

IPCC (2019) Summary for Policymakers. In: IPCC Special Report on the Ocean and Cryosphere in a Changing Climate [H.-O. Pörtner, D.C. Roberts, V. Masson-Delmotte, P. Zhai, M. Tignor, E. Poloczanska, K. Mintenbeck, A. Alegría, M. Nicolai, A. Okem, J. Petzold, B. Rama, N.M. Weyer (eds.)]. In press.

Jacob, D., Petersen, J., Eggert, B., Alias, A., Christensen, O.B., Bouwer, L.M., Braun, A., Colette, A., Déqué, M., Georgievski, G., Georgopoulou, E., Gobiet, A., Menut, L., Nikulin, G., Haensler, A., Hempelmann, N., Jones, C., Keuler, K., Kovats, S., Kröner, N., Kotlarski, S., Kriegsman, A., Martin, E., Meijgaard, E. van, Moseley, C., Pfeifer, S., Preuschmann, S., Radermacher, C., Radtke, K., Rechid, D., Rounsevell, M., Samuelsson, P., Somot, S., Soussana, J.-F., Teichmann, C., Valentini, R., Vautard, R., Weber, B., Yiou, P., 2014. EURO-CORDEX: new high-resolution climate change projections for European impact research. *Reg Environ Change* 14, 563–578. <https://doi.org/10.1007/s10113-013-0499-2>

Jacob, D., Teichmann, C., Sobolowski, S., Katragkou, E., Anders, I., Belda, M., Benestad, R., Boberg, F., Buonomo, E., Cardoso, R.M., Casanueva, A., Christensen, O.B., Christensen, J.H., Coppola, E., De Cruz, L., Davin, E.L., Dobler, A., Domínguez, M., Fealy, R., Fernandez, J., Gaertner, M.A., García-Díez, M., Giorgi, F., Gobiet, A., Goergen, K., Gómez-Navarro, J.J., Alemán, J.J.G., Gutiérrez, C., Gutiérrez, J.M., Güttler, I.,

Haensler, A., Halenka, T., Jerez, S., Jiménez-Guerrero, P., Jones, R.G., Keuler, K., Kjellström, E., Knist, S., Kotlarski, S., Maraun, D., van Meijgaard, E., Mercogliano, P., Montávez, J.P., Navarra, A., Nikulin, G., de Noblet-Ducoudré, N., Panitz, H.-J., Pfeifer, S., Piazza, M., Pichelli, E., Pietikäinen, J.-P., Prein, A.F., Preuschmann, S., Rechid, D., Rockel, B., Romera, R., Sánchez, E., Sieck, K., Soares, P.M.M., Somot, S., Srnec, L., Sørland, S.L., Termonia, P., Truhetz, H., Vautard, R., Warrach-Sagi, K., Wulfmeyer, V., 2020. Regional climate downscaling over Europe: perspectives from the EURO-CORDEX community. *Reg Environ Change* 20, 51. <https://doi.org/10.1007/s10113-020-01606-9>

Karl, T., Nicholls, N. and Ghazi, A. (eds.) (1999). *CLIVAR/GCOS/WMO workshop on indices and indicators for climate extremes: Workshop summary*. Dordrecht. Springer: Weather and Climate Extremes.

Kjellstrom, T., Holmer, I. and Lemke, B. (2009a) Workplace heat stress, health and productivity – an increasing challenge for low and middle-income countries during climate change. *Global Health Action*, 2, 2047. PMID: 20052422.

Kjellstrom, T., MSc, R. S. K., MSc, S. J. L., PhD, T. H. and PhD, R. S. J. T. (2009b) The direct impact of climate change on regional labor productivity. *Archives of Environmental & Occupational Health*, 64, 217–227. PMID: 20007118.

Kjellstrom T, Freyberg C, Lemke B, Otto M, Briggs D (2018) Estimating population heat exposure and impacts on working people in conjunction with climate change. *Int J Biometeorol* 01 3(62):291–306. <https://doi.org/10.1007/s00484-017-1407-0>

Kotlarski, S., Keuler, K., Christensen, O.B., Colette, A., Déqué, M., Gobiet, A., Goergen, K., Jacob, D., Lüthi, D., van Meijgaard, E., Nikulin, G., Schär, C., Teichmann, C., Vautard, R., Warrach-Sagi, K., Wulfmeyer, V., 2014. Regional climate modeling on European scales: a joint standard evaluation of the EURO-CORDEX RCM ensemble. *Geoscientific Model Development* 7, 1297–1333. <https://doi.org/10.5194/gmd-7-1297-2014>

Li, D., Yuan, J. and Kopp, R.E. (2020). Escalating global exposure to compound heat-humidity extremes with warming. *Environmental Research Letters*, 15, 064003

Lo, Y.T.E., Mitchell, D.M., Gasparrini, A., Vicedo-Cabrera, A.M., Ebi, K.L., Frumhoff, P.C., Millar, R.J., Roberts, W., Sera, F., Sparrow, S., Uhe, P., Williams, G. (2019) Increasing mitigation ambition to meet the Paris Agreement's temperature goal avoids substantial heat-related mortality in U.S. cities. *Sci Adv*. 5(6):eaau4373. doi: 10.1126/sciadv.aau4373. PMID: 31183397; PMCID: PMC6551192.

Matthews, T.K.R., Wilby, R.L. and Murphy, C. (2017). Communicating the deadly consequences of global warming for human heat stress. *Proceedings of the National Academy of Sciences*, 114, 3861–3866

Mora, C., Dousset, B., Caldwell, I., Powell, F., Geronimo, R., Bielecki, C., Counsell, C., Dietrich, B., Johnston, E., Louis, L., Lucas, M., McKenzie, M., Shea, A., Tseng, H., Giambelluca, T., Leon, L., Hawkins, E. and Trauernicht, C. (2017) Global risk of deadly heat. *Nature Climate Change*, 7.

Orlov A, Sillmann J, Aaheim A (2019) Economic losses of heat-induced reductions in outdoor worker productivity: a case study of Europe. *EconDisCliCha* 3:191–211. <https://doi.org/10.1007/s41885-019-00044-0>

Petitti, D. B., Hondula, D. M., Yang, S., Harlan, S. L. and Chowell, G. (2016) Multiple trigger points for quantifying heat-health impacts: New evidence from a hot climate. *Environmental Health Perspectives*, 124, 176–183.

Peterson, T.C., Folland, C., Gruza, G., Hogg, W., Mokssit, A. and Plummer, N. (2001). Report on the Activities of the Working Group on Climate Change Detection and Related Rapporteurs 1998-2001. WMO, Rep.wcdmp-47, wmo-td1071, WMO, Geneva, Switzerland.

Ragettli, M.S., Vicedo-Cabrera, A.M., Schindler, C., Roosli, M. (2017) Exploring the association between heat and mortality in Switzerland between 1995 and 2013, *Environmental Research*, 158, pp. 703-709, 10.1016/j.envres.2017.07.021

Robine, J.-M., Cheung, S. L. K., Roy, S. L., Oyen, H. V., Griths, C., Michel, J.-P. and Herrmann, F. R. (2008) Death toll exceeded 70,000 in Europe during the summer of 2003. *Comptes Rendus Biologies*, 331, 171 – 178.

Sanjay, J., Krishnan, R., Shrestha, A.B., Rajbhandari, R. and Ren, G.Y. (2017). Downscaled climate change projections for the hindukush himalayan region using cordex south asia regional climate models. *Advances in Climate Change Research*, 8, 185-198.

Schmidli, J., Goodess, M., Frei, C., Haylock, M. R., Hundscha, Y., Ribalaygua, J., and Schmith, T. (2007) Statistical and dynamical downscaling of precipitation: An evaluation and comparison of scenarios for the European Alps, *J. Geophys. Res.*, 112, D04105, doi:10.1029/2005JD007026.

Schulzweida, Uwe. (2019, October 31). CDO User Guide (Version 1.9.8). <http://doi.org/10.5281/zenodo.3539275>

Soares PMM, Cardoso RM (2017) A simple method to assess the added value using high-resolution climate distributions: application to the EURO-CORDEX daily precipitation. *Int J Climatol* 38(3):1484-1498. <https://doi.org/10.1002/joc.5261>

Taylor, K.E., Stouffer, R.J., Meehl, G.A., 2012. An Overview of CMIP5 and the Experiment Design. *Bull. Amer. Meteor. Soc.* 93, 485–498. <https://doi.org/10.1175/BAMS-D-11-00094.1>

Torma, Cs., Giorgi, F., and Coppola, E. (2015), Added value of regional climate modeling over areas characterized by complex terrain—Precipitation over the Alps, *J. Geophys. Res. Atmos.*, 120, 3957–3972. doi: 10.1002/2014JD022781.

van der Linden, P., Mitchell, J.F.B., 2009. ENSEMBLES: Climate Change and its Impacts: Summary of research and results from the ENSEMBLES project - European Environment Agency (EEA). Met Office Hadley Centre, FitzRoy Road, Exeter EX1 3PB, UK.

Zhao, Y., Ducharne, A., Sultan, B., Braconnot, P. and Vautard, R. (2015). Estimating heat stress from climate-based indicators: present-day biases and future spreads in the CMIP5 global climate model ensemble. *Environmental Research Letters*, 10, 084013.

## Appendix 1. Delta maps of indices for RCP 4.5

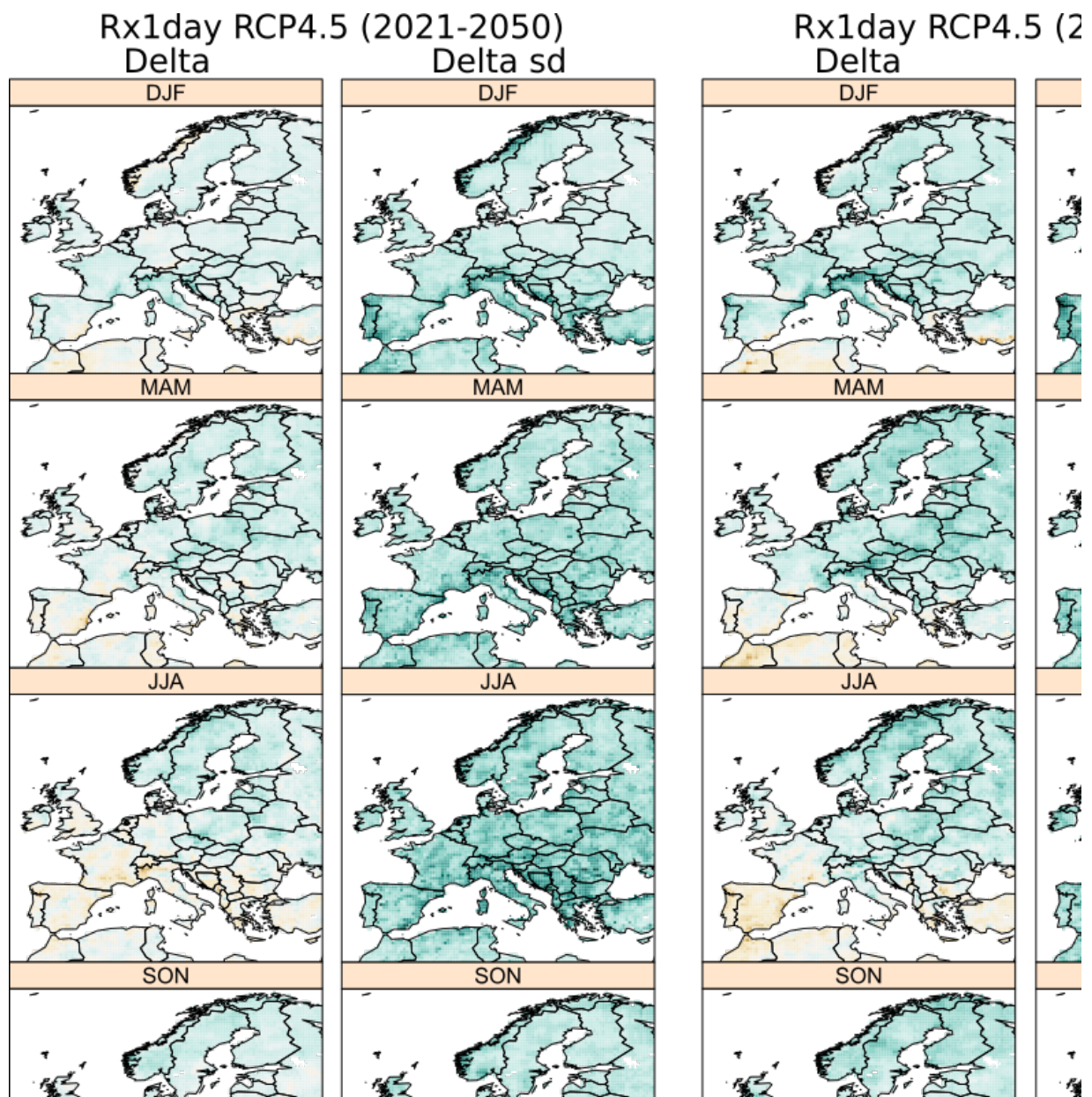


**Fig. A1.** Same as Fig. 4, but considering the RCP 4.5 scenario. The color palette range and interval has been kept identical to Fig 4 for better visual comparison.

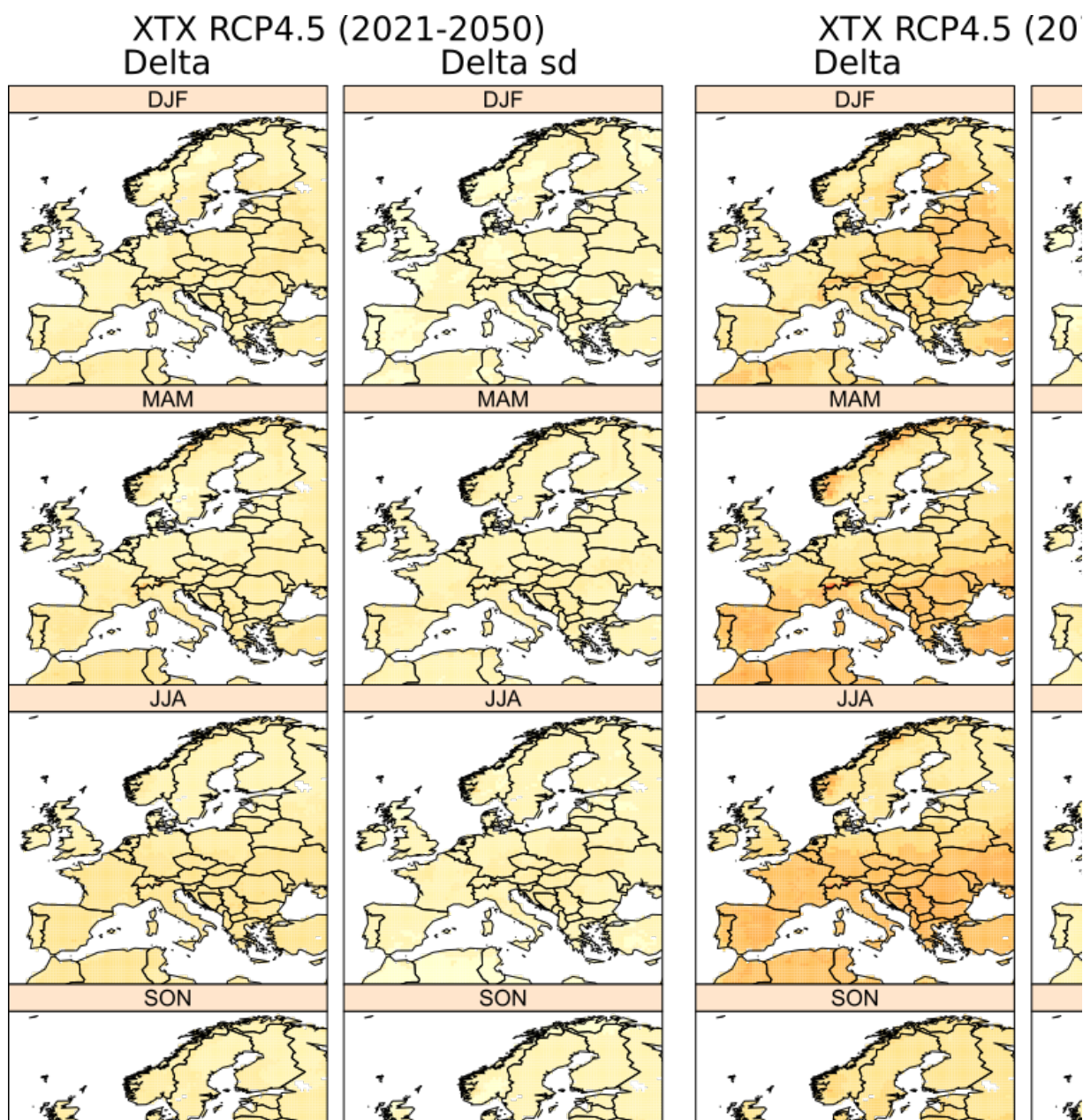


**Fig. A2.** Same as Fig. 5, but considering the RCP 4.5 scenario. The color palette range and interval has been kept identical to Fig. 5 for better visual comparison.

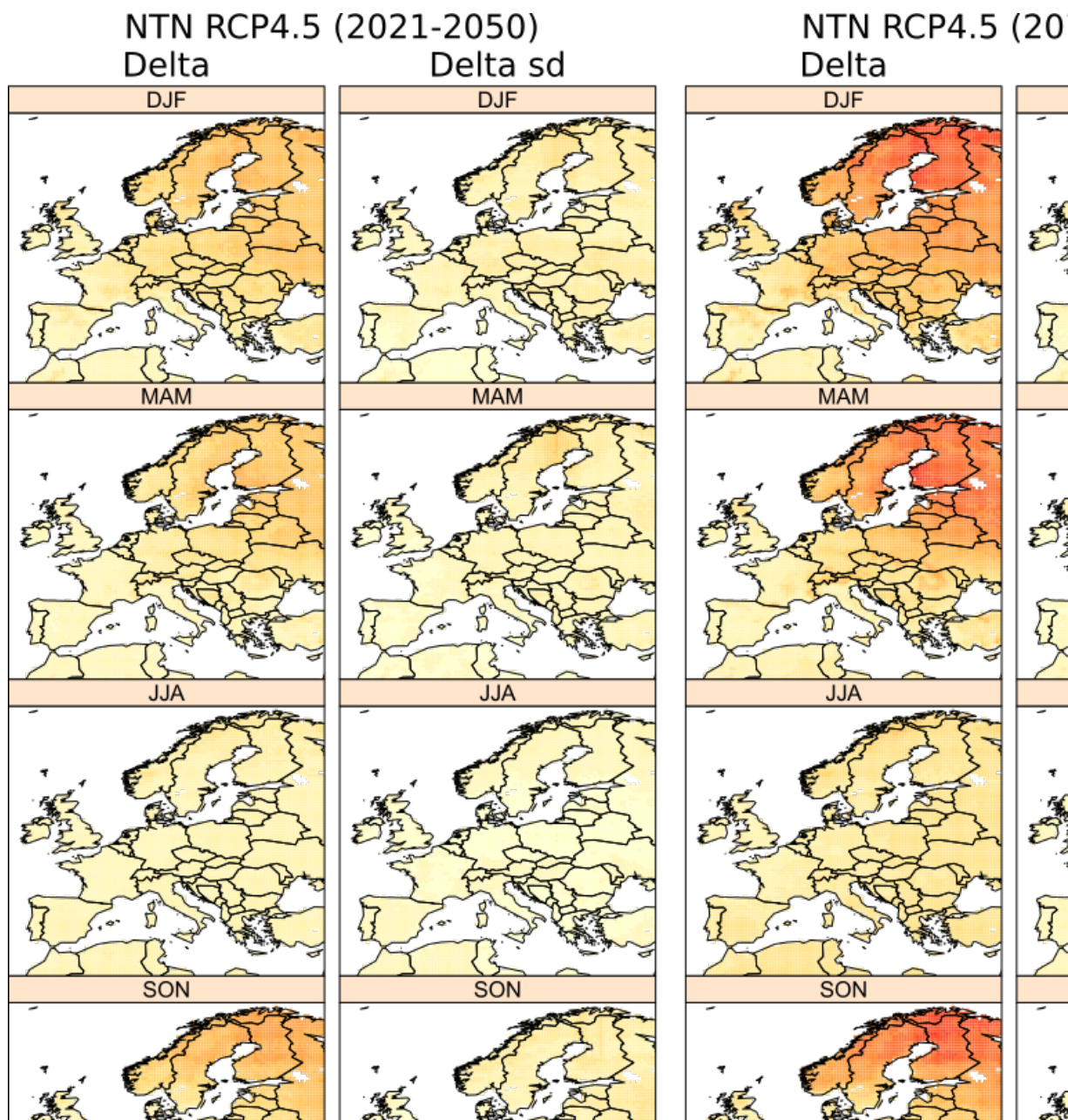


**Fig. A3.** Same as Fig. 6, but considering the RCP 4.5 scenario. The color palette range and interval has been kept identical to Fig. 5 for better visual comparison.